International Journal of Control, Automation, and Systems (2009) 7(3):419-428 http://www.springer.com/12555
DOI 10.1007/s12555-009-0311-8

Feedback Linearization vs. Adaptive Sliding Mode Control for a Quadrotor Helicopter

Daewon Lee, H. Jin Kim*, and Shankar Sastry

Abstract: This paper presents two types of nonlinear controllers for an autonomous quadrotor helicopter. One type, a feedback linearization controller involves high-order derivative terms and turns out to be quite sensitive to sensor noise as well as modeling uncertainty. The second type involves a new approach to an adaptive sliding mode controller using input augmentation in order to account for the underactuated property of the helicopter, sensor noise, and uncertainty without using control inputs of large magnitude. The sliding mode controller performs very well under noisy conditions, and adaptation can effectively estimate uncertainty such as ground effects.

Keywords: Feedback linearization, sliding mode control, UAV, quadrotor helicopter.

1. INTRODUCTION

Unmanned aerial vehicles (UAVs) are being used more often for military and civilian purposes such as traffic monitoring, patrolling for forest fires, surveillance, and rescue, in which risks to pilots are often high. Rotorcraft have an evident advantage over fixed-wing aircraft for various applications because of their vertical landing/take-off capability and payload. Among the rotorcraft, quadrotor helicopters can usually afford a larger payload than conventional helicopters due to four rotors as shown in Fig. 1. Moreover, small quadrotor helicopters possess a great maneuverability and are potentially simpler to manufacture. For these advantages, quadrotor helicopters have received much interest in UAV research.

The quadrotor we consider is an underactuated system with six outputs and four inputs, and the states are highly coupled. To deal with this system, many modeling approaches have been presented [1,2] and various control methods proposed [3-17]. First of all, several backstepping controllers have been developed. E. Altug *et al.* presented a backstepping controller using single- [3] and dual-camera [4] visual feedback. Madani *et al.* studied a full-state backstepping technique based on the Lyapunov stability theory and backstepping sliding mode control [5,6]. Yet another backstepping control method was proposed by P. Castillo *et al*. They used this controller with a saturation function and it performed well under perturbation [7]. Also, N. Metni *et al.* used backstepping techniques to derive an adaptive nonlinear tracking control law for a quadrotor system [8].

A feedback linearization controller was implemented by Altug *et al.* [3]. A PD controller was designed to y and yaw control and the feedback linearization controller was implemented to x and z control. A. Benallegue et. al. presented feedback linearization with a high-order sliding mode observer for a quadrotor and in simulation it was quite robust against wind disturbance and noise [9].

A quaternion-based feedback controller for attitude stabilization was shown in [10]. With compensation of the Coriolis and gyroscopic torques, the controller guaranteed exponential stability while a classical PD controller without compensation of the Coriolis and gyroscopic torques could guarantee only asymptotic stability. In [11], a PID controller and a LQ controller were proposed to stabilize the attitude. The PID controller showed the ability to control the attitude in the presence of minor perturbation and the LQ controller

Fig. 1. Quadrotor helicopter on a landing pad under consideration.

Manuscript received January 17, 2008; revised October 9, 2008; accepted December 31, 2008. Recommended by Editorial Board member Hyo-Choong Bang under the direction of Editor Hyun Seok Yang. This work was supported by the Korea Research Foundation Grant (MOEHRD) KRF-2005-204-D00002, the Korea Science and Engineering Foundation(KOSEF) grant funded by the Korea government(MOST) R0A-2007-000-10017-0 and Engineering Research Institute at Seoul National University.

Daewon Lee and H. Jin Kim are with School of Mechanical and Aerospace Engineering and Institute of Advanced Aerospace Technology, Seoul National University, Seoul 151-742, Korea (e-mails: {dwsh001, hjinkim}@snu.ac.kr).

Shankar Sastry is with Electrical Engineering & Computer Sciences, University of California, Berkeley, CA 94720, USA (e-mail: sastry@eecs.berkeley.edu).

* Corresponding author.

provided average results, due to model imperfections. In [12], Erginer *et al.* presented a modeling of a quadrotor helicopter system. They also proposed a PD controller to control *x*- and *y*-axis movements and altitude by actuating pitch, roll, and thrusts commands, respectively, using visual feedback.

There are also robust controllers designed for quadrotor systems. A sliding mode disturbance observer was presented in [13] to design a robust flight controller for a quadrotor vehicle. This controller allowed continuous control robust to external disturbance, model uncertainties and actuator failure. Robust adaptive-fuzzy control was applied in [14]. This controller showed a good performance against sinusoidal wind disturbance. A. Mokhtari presented robust feedback linearization with a linear generalized H-∞ controller and the results showed that the overall system was robust to uncertainties in system parameters and disturbances when weighting functions are chosen properly [15]. In [16], a robust dynamic feedback controller of Euler angles is proposed using estimates of wind parameters. This controller performed well under wind perturbation and uncertainties on inertia coefficients.

In [17], a sliding mode controller was suggested. Due to the underactuated property of a quadrotor helicopter, they divided a quadrotor system into two subsystems: a fully-actuated subsystem and an underactuated subsystem. Two separate controllers were designed for these subsystems. A PID controller was applied to the fully actuated subsystem and a sliding mode controller was designed for the underactuated subsystem. Because of the advantage of a sliding mode controller, namely insensitivity to uncertainties, it robustly stabilized the overall system under parametric uncertainties.

This study presents two nonlinear controllers for a quadrotor helicopter system. The first one operates on a feedback linearization (FL) method for an *integrated x-y-z* control. Feedback linearization controllers can be directly applied to nonlinear dynamics without linear approximations. We simplify the equation of system dynamics for the FL controller in order to avoid complex calculations involving repeated differentiation. Although this controller is simple to implement, model uncertainty can cause performance degradation or instability of the closed-loop system, because it uses inverse system dynamics as part of the control input to cancel nonlinear terms. In addition, because of the high-order derivative terms arising from the differentiation of dynamic equations, the FL controller is quite sensitive to external disturbance or sensor noise. To manage the robustness issue, we present a new approach for an adaptive sliding mode method for controlling a quadrotor helicopter using input augmentation under uncertainty and sensor noise. Sliding mode controllers are robust to bounded uncertainties such as modeling errors, sensor noise and external disturbances. However, in order to compensate for these uncertainties, sliding mode controllers tend to cause large input gains, which could be a serious limitation in power-limited systems such as small quadrotor helicopters. Adaptive sliding mode controllers can overcome the drawbacks of sliding mode controllers by adapting the estimates of uncertainty estimates, resulting in smaller input gains. In designing an adaptive sliding mode controller, we define slack variables to overcome a property of the quadrotor system that is underactuated. Furthermore, this controller is applied under uncertain conditions involving sensor noise and ground effects. Adaptation rules effectively deal with uncertainties without having to use control inputs of large magnitude.

This paper is structured as follows: In Section 2, an operating principle of a quadrotor and its dynamic equations are presented. In Section 3, a feedback linearization controller is described. Section 4 presents an adaptive sliding mode controller and error analysis for the controller. Simulation results are given in Section 5, and Section 6 contains concluding remarks.

2. QUADROTOR HELICOPTER MODEL

Quadrotor helicopters we consider have four fixed-pitch-angle blades whereas classic helicopters have variable-pitch-angle blades. The control of a quadrotor helicopter is performed by varying the speed of each rotor.

A concept of the quadrotor helicopter is shown in Fig. 2. Each rotor produces a lift force and moment. The two pairs of rotors, i.e., rotors (1,3) and rotors (2,4), rotate in opposite directions so as to cancel the moment produced by the other pair. To make a roll angle (ϕ), along the x-axis of the body frame, one can increase the angular velocity of rotor (2) and decrease the angular velocity of rotor (4) while keeping the whole thrust constant. Likewise, the angular velocity of rotor (3) is increased and the angular velocity of rotor (1) is decreased to produce a pitch angle (θ), along the y-axis of the body frame. In order to perform yawing motion (ψ), along the z-axis of the body frame, the speed of rotors (1,3) are increased and the speed of rotors (2,4) are decreased.

The quadrotor helicopter is assumed to be symmetric with respect to the *x* and *y* axes so that the center of gravity is located at the center of the quadrotor. Each rotor is located at the end of bars, whose length from the center to rotor is *l*. The rotors generate thrust force

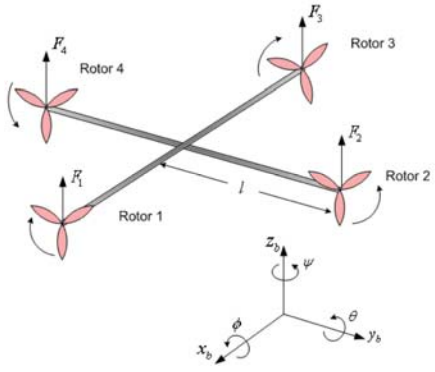

Fig. 2. A quadrotor helicopter configuration with roll-pitch-yaw Euler angles $[\phi, \theta, \psi]$.

F_i $(i=1,2,3,4)$ which are perpendicular to x-y plane as shown in Fig. 2. J_i is the moment of inertia with respect to each axis and ρ is the force-to-moment scaling factor. Then the equations of motion of the quadrotor without consideration of air drag can be presented as below.

$$\begin{bmatrix}\ddot{x}\\ \ddot{y}\\ \ddot{z}\end{bmatrix}=\frac{1}{m}(\sum_{i=1}^{4}F_i)R\vec{e_3}+(g_r(z)-g)\vec{e_3}, \tag{1}$$

$$\begin{aligned}\ddot{\phi}&=l(F_2-F_4)/J_1,\\ \ddot{\theta}&=l(-F_1+F_3)/J_2,\\ \ddot{\psi}&=\rho(F_1-F_2+F_3-F_4)/J_3.\end{aligned} \tag{2}$$

$[x,y,z]$ represent the position of the quadrotor in the inertial frame, and the attitude state variables in the body frame $[\phi,\theta,\psi]$ represent roll, pitch and yaw angles, respectively. $\vec{e_3}=[0,0,1]^T$, and R is the coordinate transformation matrix from the body frame to the inertial frame,

$$R=\begin{bmatrix}c\theta c\psi & s\phi s\theta c\psi-c\phi s\psi & c\phi s\theta c\psi+s\phi s\psi\\ c\theta s\psi & s\phi s\theta s\psi+c\phi c\psi & c\phi s\theta s\psi-s\phi c\psi\\ -s\theta & s\phi c\theta & c\phi c\theta\end{bmatrix},$$

where c and s denote cosine and sine functions, respectively, and g denotes gravity.

The term $g_r(z)$ represents the ground effect during landing. As shown in (3), we assumed that the ground effect affects the UAV when the UAV is below the certain altitude, z_0 [19].

$$g_r(z)=\begin{cases}\dfrac{A}{(z+z_{cg})^2}-\dfrac{A}{(z_0+z_{cg})^2} & 0<z\le z_0\\ 0 & \text{else}\end{cases} \tag{3}$$

where A is the ground effect constant and z_{cg} is the z component of the center of gravity. Because it is very difficult to derive the exact equations for the ground effect, the term $g_r(z)$ is considered an unknown perturbation in designing a controller, which requires compensation or adaptation.

In order to simplify (1) and (2), input terms are defined as (4). u_1 is the normalized total lift force, and u_2, u_3 and u_4 correspond to the control inputs of roll, pitch and yaw moments, respectively.

$$\begin{aligned}u_1&=(F_1+F_2+F_3+F_4)/m,\\ u_2&=(F_2-F_4)/J_1,\\ u_3&=(-F_1+F_3)/J_2,\\ u_4&=\rho(F_1-F_2+F_3-F_4)/J_3.\end{aligned} \tag{4}$$

Then the equations of motion can be represented as (5)-(10):

$$\ddot{x}=u_1(\cos\phi\sin\theta\cos\psi+\sin\phi\sin\psi), \tag{5}$$

$$\ddot{y}=u_1(\cos\phi\sin\theta\sin\psi-\sin\phi\cos\psi), \tag{6}$$

$$\ddot{z}=u_1(\cos\phi\cos\theta)-g+g_r(z), \tag{7}$$

$$\ddot{\phi}=u_2 l, \tag{8}$$

$$\ddot{\theta}=u_3 l, \tag{9}$$

$$\ddot{\psi}=u_4\ , \tag{10}$$

or, equivalently, using $\mathbf{x}=[x,y,z,\phi,\theta,\psi]^T$ and $\mathbf{u}=[u_1,u_2,u_3,u_4]^T$, in the vector form as (11).

$$\ddot{\mathbf{x}}=f(\mathbf{x})+g(\mathbf{x})\mathbf{u}+f_r(\mathbf{x}), \tag{11}$$

$$f(\mathbf{x})=\begin{bmatrix}0\\0\\-g\\0\\0\\0\end{bmatrix},\ f_r(\mathbf{x})=\begin{bmatrix}0\\0\\g_r(z)\\0\\0\\0\end{bmatrix},$$

$$g(\mathbf{x})=\begin{bmatrix}\cos\phi\sin\theta\cos\psi+\sin\phi\sin\psi & 0 & 0 & 0\\ \cos\phi\sin\theta\sin\psi-\sin\phi\cos\psi & 0 & 0 & 0\\ \cos\phi\cos\theta & 0 & 0 & 0\\ 0 & l & 0 & 0\\ 0 & 0 & l & 0\\ 0 & 0 & 0 & 1\end{bmatrix}.$$

3. FEEDBACK LINEARIZATION CONTROL

A feedback linearization method for x-y-z control of a quadrotor helicopter system is presented in this section. The feedback linearization transforms a nonlinear system into an equivalent linear system so that we can handle the system easily.

3.1. The feedback linearization structure

Feedback linearization (FL), one of the most popular control methods for nonlinear systems, is employed in this section. However the quadrotor under consideration is an underactuated system, and $g(\mathbf{x})$ in (11) is not invertible. So the nonlinear terms in (11) cannot be directly canceled by inverting $g(\mathbf{x})$. To make this system feedback linearizable, one may consider choosing z,ϕ,θ and ψ as output variables. Then, zero dynamics of this system can be written as (12) and (13):

$$\begin{aligned}\ddot{x}&=g\left(\frac{\cos\phi\sin\theta\cos\psi}{\cos\phi\cos\theta}+\frac{\sin\phi\sin\psi}{\cos\phi\cos\theta}\right)\\ &=g\left(\tan\theta\cos\psi+\frac{\sin\psi}{\cos\theta}\tan\phi\right)\approx g\tan\theta,\end{aligned} \tag{12}$$

$$\begin{aligned}\ddot{y}&=g\left(\frac{\cos\phi\sin\theta\sin\psi}{\cos\phi\cos\theta}-\frac{\sin\phi\cos\psi}{\cos\phi\cos\theta}\right)\\ &=g\left(\tan\theta\sin\psi-\frac{\cos\psi}{\cos\theta}\tan\phi\right)\approx -g\frac{\tan\phi}{\cos\theta}.\end{aligned} \tag{13}$$

As the full analysis of the exact zero dynamics is rather complex, the above approximations are obtained by setting $|\psi| \ll 1$, and the approximated zero dynamics are unstable. This approximation can be supported by the small values of $|\psi|$ in the simulation results [3].

On the other hand, if x, y, z and ψ are chosen as output variables, it can be easily seen that u_2 and u_3 do not appear in (5), (6), (7), and (10), so we need to differentiate these equations until the input terms appear. Because of the repeated differentiation, the FL controller design involves complex computation and several derivative terms that are quite sensitive to noise. In order to reduce the number of complicated derivative terms involved in further differentiations of x and y, we first approximate (5)-(10), into (14)-(19) using the small-angle assumption while ignoring the ground effect.

$$\ddot{x} = u_1 \sin\theta, \tag{14}$$

$$\ddot{y} = -u_1 \sin\phi, \tag{15}$$

$$\ddot{z} = u_1 \cos\phi \cos\theta - g, \tag{16}$$

$$\ddot{\phi} = u_2 l, \tag{17}$$

$$\ddot{\theta} = u_3 l, \tag{18}$$

$$\ddot{\psi} = u_4. \tag{19}$$

The behavior of the remaining state variables ϕ and θ after the x - y - z and ψ control depend only on the control inputs u_2 and u_3, and their responses will be checked by simulations.

3.2. x - y - z and ψ controller design

To obtain the input of the x - y - z controller, we differentiate (14), (15), and (16) until the input terms appear. The input terms, $u_2 (= \ddot{\phi}/l)$ and $u_3 (= \ddot{\theta}/l)$, appear in the second derivatives of (14), (15), and (16), which are (20), (21), and (22), respectively.

$$\begin{aligned} x^{(3)} &= \dot{u}_1 \sin\theta + u_1 \dot{\theta} \cos\theta, \\ x^{(4)} &= \ddot{u}_1 \sin\theta + 2\dot{u}_1 \dot{\theta} \cos\theta - u_1 \dot{\theta}^2 \sin\theta + u_1 \ddot{\theta} \cos\theta, \end{aligned} \tag{20}$$

$$\begin{aligned} y^{(3)} &= -\dot{u}_1 \sin\phi - u_1 \dot{\phi} \cos\phi, \\ y^{(4)} &= -\ddot{u}_1 \sin\phi - 2\dot{u}_1 \dot{\phi} \cos\phi + u_1 \dot{\phi}^2 \sin\phi - u_1 \ddot{\phi} \cos\phi, \end{aligned} \tag{21}$$

$$\begin{aligned} z^{(3)} &= \dot{u}_1 \cos\theta \cos\phi - u_1 \dot{\theta} \sin\theta \cos\phi - u_1 \dot{\phi} \cos\theta \cos\phi, \\ z^{(4)} &= -2\dot{u}_1 \dot{\theta} \sin\theta \cos\phi - 2\dot{u}_1 \dot{\phi} \cos\theta \sin\phi \\ &\quad + 2u_1 \dot{\theta}\dot{\phi} \sin\theta \sin\phi - u_1 (\dot{\theta}^2 + \dot{\phi}^2) \cos\theta \cos\phi \\ &\quad + \ddot{u}_1 \cos\theta \cos\phi - u_1 \ddot{\theta} \sin\theta \cos\phi - u_1 \ddot{\phi} \cos\theta \sin\phi. \end{aligned} \tag{22}$$

We define an extended system which includes an additional input $\ddot{u}_1$, then the control inputs generated by the x - y - z controller are $[\ddot{u}_1, u_2, u_3]^T$. Equations (20)-(22) are rewritten in the matrix form shown in (23), and the control inputs are defined as (24) using pseudo inputs $[v_1, v_2, v_3]$.

Setting the pseudo input terms as

$$\begin{aligned} v_1 &= x_d^{(4)} - k_{x1} e_x^{(3)} - k_{x2} \ddot{e}_x - k_{x3} \dot{e}_x - k_{x4} e_x, \\ v_2 &= y_d^{(4)} - k_{y1} e_y^{(3)} - k_{y2} \ddot{e}_y - k_{y3} \dot{e}_y - k_{y4} e_y, \\ v_3 &= z_d^{(4)} - k_{z1} e_z^{(3)} - k_{z2} \ddot{e}_z - k_{z3} \dot{e}_z - k_{z4} e_z \end{aligned}$$

yields

$$\begin{aligned} e_x^{(4)} + k_{x1} e_x^{(3)} + k_{x2} \ddot{e}_x + k_{x3} \dot{e}_x + k_{x4} e_x &= 0, \\ e_y^{(4)} + k_{y1} e_y^{(3)} + k_{y2} \ddot{e}_y + k_{y3} \dot{e}_y + k_{y4} e_y &= 0, \\ e_z^{(4)} + k_{z1} e_z^{(3)} + k_{z2} \ddot{e}_z + k_{z3} \dot{e}_z + k_{z4} e_z &= 0, \end{aligned}$$

where $e_x := x - x_d$, $e_y := y - y_d$, and $e_z := z - z_d$. We can choose gains $[k_{x1}, \cdots, k_{x4}]$, $[k_{y1}, \cdots, k_{y4}]$ and $[k_{z1}, \cdots, k_{z4}]$ to obtain stable error dynamics for the simplified system. And the ψ -controller is a PD

$$\begin{bmatrix} x^{(4)} \\ y^{(4)} \\ z^{(4)} \end{bmatrix} = \begin{bmatrix} 2\dot{u}_1 \dot{\theta} \cos\theta - u_1 \dot{\theta}^2 \sin\theta \\ -2\dot{u}_1 \dot{\phi} \cos\phi + u_1 \dot{\phi}^2 \sin\phi \\ -2\dot{u}_1 \dot{\theta} \sin\theta \cos\phi - 2\dot{u}_1 \dot{\phi} \cos\theta \sin\phi + 2u_1 \dot{\theta}\dot{\phi} \sin\theta \sin\phi - u_1 (\dot{\theta}^2 + \dot{\phi}^2) \cos\theta \cos\phi \end{bmatrix} + \begin{bmatrix} \sin\theta & u_1 \cos\theta & 0 \\ -\sin\phi & 0 & -u_1 \cos\phi \\ \cos\theta \cos\phi & -u_1 \sin\theta \cos\phi & -u_1 \cos\theta \sin\phi \end{bmatrix} \begin{bmatrix} \ddot{u}_1 \\ u_2 \\ u_3 \end{bmatrix}, \tag{23}$$

$$\begin{bmatrix} \ddot{u}_1 \\ u_2 \\ u_3 \end{bmatrix} = \begin{bmatrix} \sin\theta & u_1 \cos\theta & 0 \\ -\sin\phi & 0 & -u_1 \cos\phi \\ \cos\theta \cos\phi & -u_1 \sin\theta \cos\phi & -u_1 \cos\theta \sin\phi \end{bmatrix}^{-1} \cdot \begin{bmatrix} -2\dot{u}_1 \dot{\theta} \cos\theta + u_1 \dot{\theta}^2 \sin\theta + v_1 \\ 2\dot{u}_1 \dot{\phi} \cos\phi - u_1 \dot{\phi}^2 \sin\phi + v_2 \\ 2\dot{u}_1 \dot{\theta} \sin\theta \cos\phi + 2\dot{u}_1 \dot{\phi} \cos\theta \sin\phi - 2u_1 \dot{\theta}\dot{\phi} \sin\theta \sin\phi + u_1 (\dot{\theta}^2 - \dot{\phi}^2) \cos\theta \cos\phi + v_3 \end{bmatrix}. \tag{24}$$

controller:

$$u_4 = \ddot{\psi}_d + k_{\psi 1}(\dot{\psi}_d - \dot{\psi}) + k_{\psi 2}(\psi_d - \psi), \quad (25)$$

where $k_{\psi 1}$ and $k_{\psi 2}$ are derivative and proportional gains, respectively.

4. SLIDING MODE CONTROL

This section describes an adaptive sliding mode controller. We define a suitable sliding surface and adaptation rules so that a trajectory of the system follows desired references under ground effects and noisy sensors [18].

4.1. Adaptive sliding mode control with augmented inputs

Since $g(\mathbf{x})$ is a 6-by-4 matrix, $g(\mathbf{x})$ of (11) is not invertible as mentioned previously. By augmenting slack variables $\mathbf{g}_s$ to $g(\mathbf{x})$ and $\mathbf{u}_s$ to $\mathbf{u}$ in order to form a square system, we can rewrite the system dynamics of (11) as

$$\ddot{\mathbf{x}} = f(\mathbf{x}) + G(\mathbf{x})U - \nu + f_r(\mathbf{x}), \quad (26)$$

where $G = [g(\mathbf{x}), \mathbf{g}_s]$, $U = [\mathbf{u}^T, \mathbf{u}_s^T]^T$, and $\nu = \mathbf{g}_s \mathbf{u}_s$. $\mathbf{g}_s$ is set to be constant and defined in advance to make $G(\mathbf{x})$ invertible, and $\mathbf{u}_s = [u_5, u_6]^T$ are the slack variables. If we set

$$\mathbf{g}_s = \begin{bmatrix} 1 & 0 & 0 & 0 & 0 & 0 \\ 0 & 1 & 0 & 0 & 0 & 0 \end{bmatrix}^T, \quad (27)$$

then $\nu = \mathbf{g}_s \mathbf{u}_s = \begin{bmatrix} u_5 & u_6 & 0 & 0 & 0 & 0 \end{bmatrix}^T$, so we need to estimate the slack variables u_5 and u_6. In this case, we have

$$G^{-1}(\mathbf{x}) \approx \begin{bmatrix} 0 & 0 & 1 & 0 & 0 & 0 \\ 0 & 0 & 0 & 1/I & 0 & 0 \\ 0 & 0 & 0 & 0 & 1/I & 0 \\ 0 & 0 & 0 & 0 & 0 & 1 \\ 1 & 0 & 0 & 0 & 0 & 0 \\ 0 & 1 & 0 & 0 & 0 & 0 \end{bmatrix},$$

when the small-angle assumption holds.

Let $\mathbf{e} = \mathbf{x} - \mathbf{x}_d$ denote the error vector with respect to the vector of desired state variables $\mathbf{x}_d = [x_d, y_d, z_d, \phi_d, \theta_d, \psi_d]^T$, and define the sliding surface as

$$S = [s_1, s_2, s_3, s_4, s_5, s_6]^T = \dot{\mathbf{e}} + K\mathbf{e}, \quad (28)$$

where $K = diag[k_1, \cdots, k_6]$ is a diagonal matrix with positive entries, so that the trajectory of the system could follow the desired references on the sliding surface S = **0**.

In order to cancel nonlinear terms in (26), we need to define the estimated values of ν and $f_r(\mathbf{x})$, which we denote as $\hat{\nu}$ and $\hat{f}_r(\mathbf{x})$, respectively. Let us define $\tilde{\nu} := \nu - \hat{\nu}$ and $\tilde{f}_r(\mathbf{x}) := f_r(\mathbf{x}) - \hat{f}_r(\mathbf{x})$, and let the Lyapunov function be

$$L = \frac{1}{2} S^T S + \frac{1}{2} \tilde{\nu}^T \Gamma \tilde{\nu} + \frac{1}{2} \tilde{f}_r(\mathbf{x})^T \Omega \tilde{f}_r(\mathbf{x}), \quad (29)$$

where Γ and Ω are positive semidefinite weighting matrices.

Let us assume that ν and $f_r(\mathbf{x})$ change slowly enough, which leads to $\dot{\tilde{\nu}} \approx -\dot{\hat{\nu}}$ and $\dot{\tilde{f}}_r(\mathbf{x}) \approx -\dot{\hat{f}}_r(\mathbf{x})$. Then the first-order derivative of the Lyapunov function can be derived as

$$\begin{aligned} \dot{L} &= S^T \dot{S} + \tilde{\nu}^T \Gamma \dot{\tilde{\nu}} + \tilde{f}_r(\mathbf{x})^T \Omega \dot{\tilde{f}}_r(\mathbf{x}) \\ &= S^T [f(x) + G(x)U - \nu + f_r(\mathbf{x}) - \ddot{\mathbf{x}}_d + K\dot{\mathbf{e}}] \\ &\quad + \tilde{\nu}^T \Gamma(-\dot{\hat{\nu}}) + \tilde{f}_r(\mathbf{x})^T \Omega(-\dot{\hat{f}}_r(\mathbf{x})). \end{aligned} \quad (30)$$

To make the first-order derivative of Lyapunov function negative definite, the augmented input U is selected as (31):

$$\begin{aligned} U = G^{-1}(x)[&-f(x) + \hat{\nu} - \hat{f}_r(\mathbf{x}) \\ &+ \ddot{\mathbf{x}}_d - K\dot{\mathbf{e}} - diag[c_1, \cdots, c_6] sign(S^T)]. \end{aligned} \quad (31)$$

Then (30) becomes

$$\dot{L} = \tilde{\nu}^T [-S - \Gamma \dot{\hat{\nu}}] + \tilde{f}_r(\mathbf{x})^T [S - \Omega \dot{\hat{f}}_r(\mathbf{x})] - C^T |S|, \quad (32)$$

where $C = [c_1, c_2, c_3, c_4, c_5, c_6]^T$ is an input gain vector. So we can update $\dot{\hat{\nu}}$ and $\dot{\hat{f}}_r(\mathbf{x})$ as

$$\dot{\hat{\nu}} = -\begin{bmatrix} \dot{e}_x + k_1 e_x, \dot{e}_y + k_2 e_y, 0, 0, 0, 0 \end{bmatrix}^T, \quad (33)$$

$$\dot{\hat{f}}_r(\mathbf{x}) = \begin{bmatrix} 0, 0, & \dot{e}_z + k_3 e_z, 0, 0, 0 \end{bmatrix}^T. \quad (34)$$

And with positive entries of C, we can make (30) as

$$\dot{L} = -C^T |S| < 0,$$

which means S→**0**.

In order to check the steady state of the estimated variables under this adaptive sliding mode controller, we combine (26) and (31) with $S \approx 0$, $\dot{S} \approx 0$, which yields

$$\nu - \hat{\nu} \approx f_r - \hat{f}_r, \quad (35)$$

$$\text{i.e.,} \begin{bmatrix} u_5 - \hat{u}_5 \\ u_6 - \hat{u}_6 \\ 0 \\ 0 \\ 0 \\ 0 \end{bmatrix} = \begin{bmatrix} 0 \\ 0 \\ g_r - \hat{g}_r \\ 0 \\ 0 \\ 0 \end{bmatrix}.$$

Thus, the estimations $\hat{u}_5$, $\hat{u}_6$, and $\hat{g}_r$ will converge to its true values in steady state.

In (31), the dominant terms for u_1, u_2, u_3 and u_4 are $[\dot{e}_z, e_z]$, $[\dot{e}_\phi, e_\phi]$, $[\dot{e}_\theta, e_\theta]$ and $[\dot{e}_\psi, e_\psi]$, and we cannot control the x and y states directly from the inputs. So we define the desired values for ϕ and θ as (36) and (37) to control the x and y positions.

$$\phi_d = \dot{e}_y + k_\phi\, e_y, \tag{36}$$

$$\theta_d = \dot{e}_x + k_\theta\, e_x. \tag{37}$$

Here k_ϕ and k_θ are proportional gains.

4.2. Advantage of adaptive sliding mode controller: input magnitude point of view

We can determine the value of C to satisfy (38) from the combination of (30), (33), and (34).

$$\dot{L} = S^T \begin{bmatrix} -C_1 sign|S_1| \\ -C_2 sign|S_2| \\ -C_3 sign|S_3| \\ -C_4 sign|S_4| \\ -C_5 sign|S_5| \\ -C_6 sign|S_6| \end{bmatrix} < 0. \tag{38}$$

If we use the standard sliding mode control rather than performing the adaptation for the slack variable ν and the ground effect f_r as in (33)-(34), the uncertain terms u_5, u_6 and g_r will be contained in the first, second and third rows, respectively, of the matrix in (38) as below:

$$\dot{L}_{non-adaptive} = S^T \begin{bmatrix} -u_5 - C_1 sign|S_1| \\ -u_6 - C_2 sign|S_2| \\ g_r - C_3 sign|S_3| \\ -C_4 sign|S_4| \\ -C_5 sign|S_5| \\ -C_6 sign|S_6| \end{bmatrix} < 0. \tag{39}$$

Thus, in the non-adaptive case, it would be necessary to use the input gains, C_1, C_2 and C_3, large enough to compensate $|u_5|, |u_6|$ and $|g_r|$ to make $\dot{L}_{non-adaptive} < 0$. One can notice from the comparison of (38) and (39) that the adaptive sliding mode controller requires smaller input magnitude, which is a clear advantage in terms of reduced chattering and power efficiency.

4.3. Sensor noise analysis in adaptive sliding mode control

In our experimental setup, we use a vision sensor to estimate the position and attitude information, which causes calibration error as written in (40).

$$E = [\varepsilon_x \quad \varepsilon_y \quad \varepsilon_z \quad \varepsilon_\phi \quad \varepsilon_\theta \quad \varepsilon_\psi]^T \tag{40}$$

So the measured state variables $\hat{X}$ are given as (41).

$$\hat{X} = X + E \tag{41}$$

Since the calibration error terms affect e_x and e_y, ϕ_d and θ_d in (36) and (37) involves the calibration error terms. So the desired state vector includes those error terms as shown in (42). Now let η_* denote error terms included in $*$. Then the desired state has error terms as shown in (42), and for example, $\eta_{\mathbf{X}\,d}$ can be defined as (43).

$$\hat{X}_d = \begin{bmatrix} x_d \\ y_d \\ z_d) \\ (\dot{y} + \dot{\varepsilon}_y - \dot{y}_d + k_\phi (y + \varepsilon_y - y_d)) \\ (\dot{x} + \dot{\varepsilon}_x - \dot{x}_d + k_\theta (x + \varepsilon_x - x_d)) \\ \psi_d \end{bmatrix}, \tag{42}$$

$$\eta_{X\,d} = \begin{bmatrix} 0 \\ 0 \\ 0 \\ \dot{\varepsilon}_y + k_\phi \varepsilon_y \\ \dot{\varepsilon}_x + k_\theta \varepsilon_x \\ 0 \end{bmatrix}. \tag{43}$$

Therefore, $\eta_{\ddot{\mathbf{X}}_d}$ and $\eta_{\dot{e}}$ can be derived as

$$\eta_{\ddot{\mathbf{X}}_d} = \begin{bmatrix} 0 \\ 0 \\ 0 \\ \varepsilon_y^{(3)} + k_\phi \ddot{\varepsilon}_y \\ \varepsilon_x^{(3)} + k_\theta \ddot{\varepsilon}_x \\ 0 \end{bmatrix}, \quad \eta_{\dot{e}} = \dot{E}. \tag{44}$$

Recalling (31) about the input U, the error terms included in U can be expressed as the following:

$$\eta_U = G(\mathbf{X})^{-1} \begin{bmatrix} -k_1 \dot{\varepsilon}_x \\ -k_2 \dot{\varepsilon}_y \\ -k_3 \dot{\varepsilon}_z \\ \varepsilon_y^{(3)} + k_\phi \ddot{\varepsilon}_y - k_4 \dot{\varepsilon}_\phi \\ \varepsilon_x^{(3)} + k_\theta \ddot{\varepsilon}_x - k_5 \dot{\varepsilon}_\theta \\ -k_6 \dot{\varepsilon}_\psi \end{bmatrix}.$$

We used a saturation function and a first order filter to limit the jump in U caused by the error terms of $\left[\dot{\varepsilon}_x \quad \dot{\varepsilon}_y \quad \dot{\varepsilon}_z \quad \dot{\varepsilon}_\phi \quad \dot{\varepsilon}_\theta \quad \dot{\varepsilon}_\psi \quad \ddot{\varepsilon}_x \quad \ddot{\varepsilon}_y \quad \varepsilon_x^{(3)} \quad \varepsilon_y^{(3)}\right]$.

5. SIMULATION RESULTS

The proposed FL controller and adaptive sliding mode controller for the quadrotor helicopter are tested here in simulations. The ground effect and sensor noise are omitted in the first simulation using the FL controller. Two different simulations were performed for the adaptive sliding mode controller: 1) excluding sensor noise and 2) including sensor noise, while the ground effect was included in both simulations. In order to reduce the chattering caused by $sign(S)$, S was used in simulation instead of $sign(S)$. Parameter settings for those simulations are:

$$
\begin{aligned}
&J_1 = J_2 = 2\ \text{Ns}^2/\text{rad},\\
&J_3 = 3\ \text{Ns}^2/\text{rad},\\
&m = 2.5\ \text{kg},\\
&l = 1\ \text{m},\\
&g = 9.81\ \text{m}/s^2,\\
&A = 0.4668,\\
&z_0 = 2\ \text{m},\\
&\Gamma = diag\begin{bmatrix}1 & 1 & 0 & 0 & 0 & 0\end{bmatrix},\\
&\Omega = diag\begin{bmatrix}0 & 0 & 1 & 0 & 0 & 0\end{bmatrix},\\
&C = [5,\ 5,\ 5,\ 1,\ 1,\ 1]^T,\\
&K = diag\begin{bmatrix}1 & 1 & 0.7 & 5 & 5 & 10\end{bmatrix},\\
&k_\phi = k_\theta = 5,\\
&x(0) = 10\ \text{m},\ y(0) = 10\ \text{m},\ z(0) = 20\ \text{m},\\
&\phi(0) = 30\ \text{deg},\ \theta(0) = 30\ \text{deg},\ \psi(0) = 30\ \text{deg}.
\end{aligned}
\tag{45}
$$

A mission of the UAV is to land at origin (0,0,0) from the starting point (10,10,20) via waypoint (20,-10,10). To land safely, extra care has been taken so that the altitude profile does not contain any overshoot.

Simulation results of the FL controller without sensor noise are presented first. The gains of FL controller, $[k_{x1},\cdots,k_{x4}]^T$, $[k_{y1},\cdots,k_{y4}]^T$, and $[k_{z1},\cdots,k_{z4}]^T$ are obtained from the LQR (Linear quadratic regulator) method:

$$J(u) = \int_0^\infty (x^T Q x + u^T R u)dt, \tag{46}$$

where $Q = diag[1,\ 10,\ 5,\ 1]$, $R = 0.01$, which yields

$$\begin{bmatrix}k_{x1}\\ \vdots \\ k_{x4}\end{bmatrix} = \begin{bmatrix}k_{y1}\\ \vdots \\ k_{y4}\end{bmatrix} = \begin{bmatrix}k_{z1}\\ \vdots \\ k_{z4}\end{bmatrix} = \begin{bmatrix}10.00\\ 42.49\\ 40.27\\ 13.43\end{bmatrix}.$$

Fig. 3 shows the resulting three-dimensional trajectory of the UAV without the ground effect term and sensor noise, and Fig. 4 shows the six state variables of the helicopter while it moves from (10,10,20) to (0,0,0) via

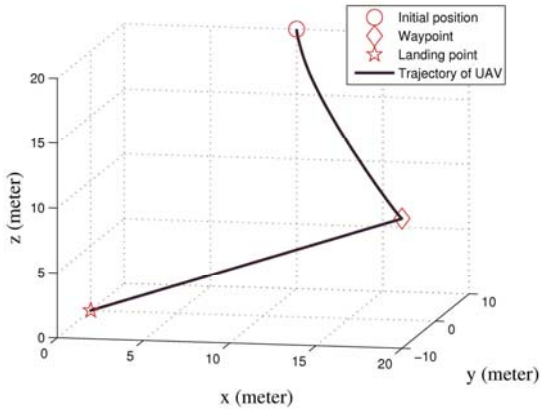

Fig. 3. Trajectory of UAV in 3-D axes with FL controller without uncertainty and sensor noise.

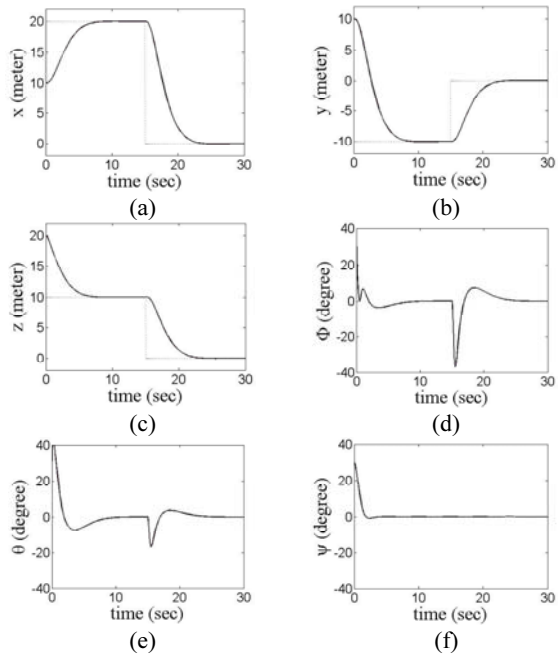

Fig. 4. FL controller results without uncertainty and sensor noise. (a),(b),(c): x, y, z positions. (d), (e),(f): roll, pitch, yaw angles (solid: state variables of UAV, dotted: desired values).

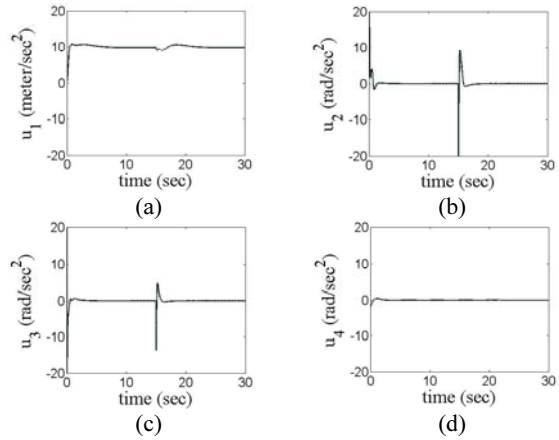

Fig. 5. Inputs generated by the FL controller without uncertainty and sensor noise.

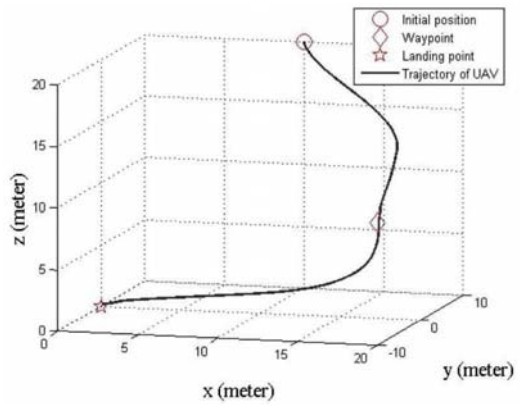

Fig. 6. Trajectory of UAV in 3-D axes with the adaptive sliding mode controller with uncertainty but without sensor noise.

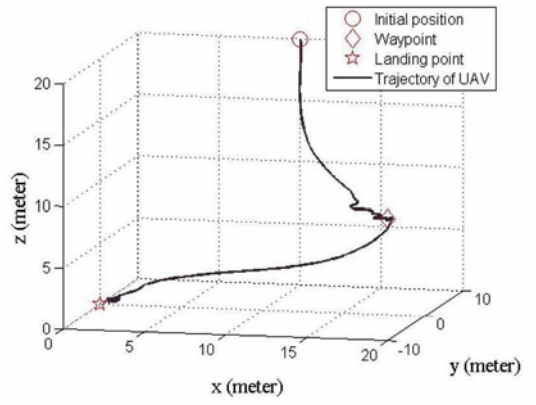

Fig. 9. Trajectory of UAV in 3-D axes with the adaptive sliding mode controller with uncertainty and sensor noise.

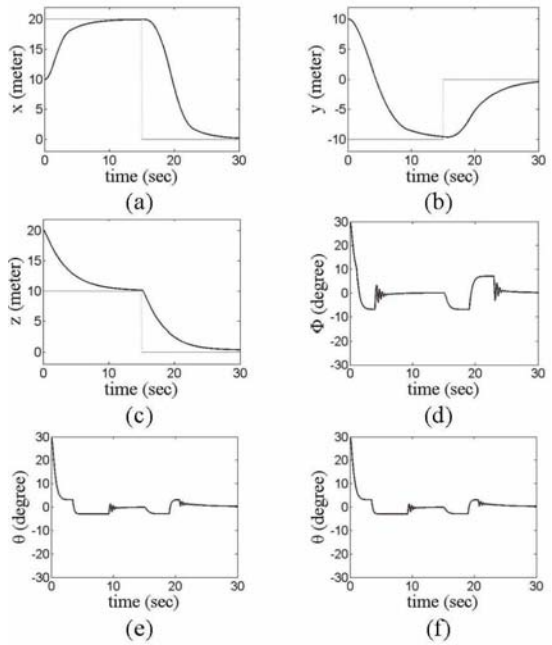

Fig. 7. Positions and attitudes using the adaptive sliding mode controller with uncertainty but without sensor noise.

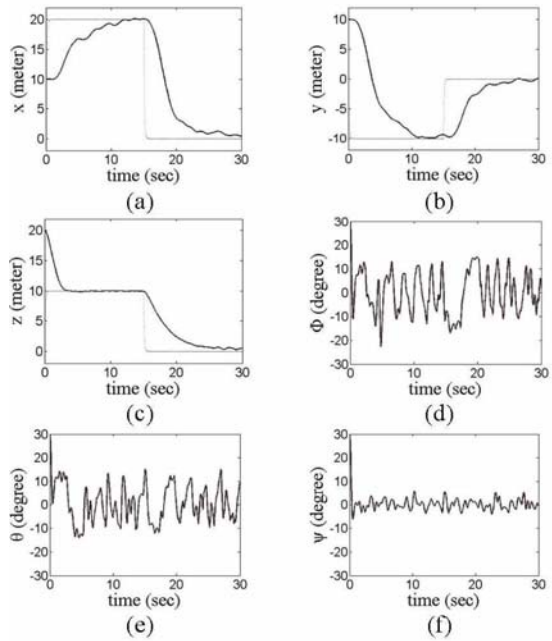

Fig. 10. Positions and attitudes using the adaptive sliding mode controller with uncertainty and sensor noise.

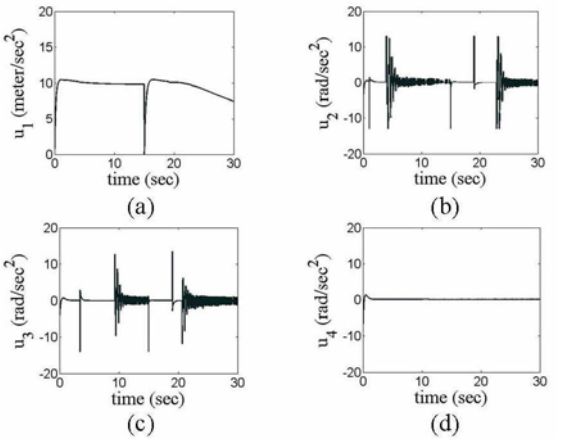

Fig. 8. Inputs generated by the adaptive sliding mode controller with uncertainty but without sensor noise.

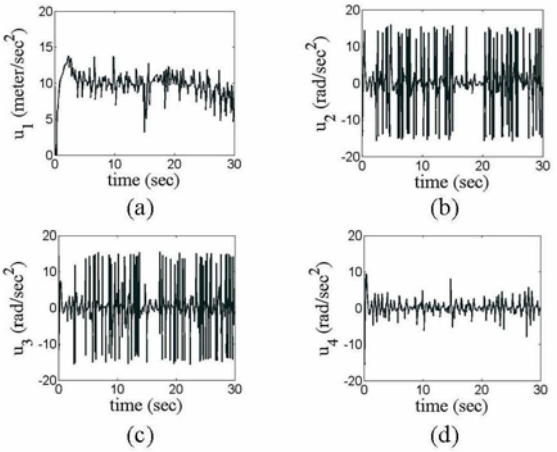

Fig. 11. Inputs generated by the adaptive sliding mode controller with uncertainty and sensor noise.

(20,-10,10) with given initial pitch, roll and yaw angles. The control inputs are shown in Fig. 5. Since we chose the output of the FL method to be x, y, z and ψ, the remaining variables ϕ and θ can be considered the internal dynamics under the FL controller, and Fig. 4 shows that the internal dynamics of FL controller are stable.

The results of the adaptive sliding mode controller without sensor noise are shown in Figs. 6-8. As shown in the ϕ and θ plots in Fig. 7, chattering occurs even when sensor noise does not exist, this is because we use the e_x and e_y to compute the ϕ_d and θ_d as written in (36) and (37).

As we can see in Figs. 3-5, the feedback-linearization controller yields a satisfactory result when there is no noise. Although the sliding mode controller also performs well, the feedback linearization uses more efficient inputs without chattering, when compared with the sliding mode controller (Fig. 4 vs. Fig. 7, and Fig. 5 vs. Fig. 8).

However, with uncertainty and sensor noise, the FL controller does not guarantee the stability, and the resulting trajectory and state variables diverge. This is because the FL controller requires higher-order derivative terms of states to compute the inputs in our quadrotor example and relies on exact information on the dynamic equations.

Results under the adaptive sliding mode controller considering uncertainty and sensor noise are shown in Figs. 9 -11. Sensor noise is applied to six state variables. Mean and standard deviation of each noise are $0\,\mathrm{m}$ and $0.05\,\mathrm{m}$ for x, y and z, and $0.01\,\mathrm{rad}$ for ϕ, θ and ψ. Although there is chattering around the desired trajectory, the adaptive sliding mode controller robustly completes the mission under uncertainty and sensor noise as we can see in Figs. 9 and 10. And as shown in Fig. 11, chattering in the input channels suppresses the sensor noise.

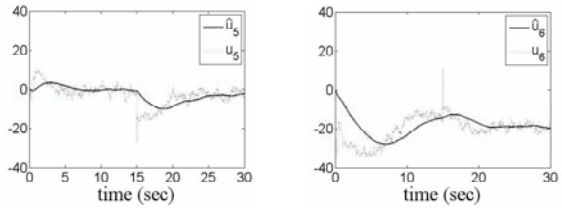

(a) (b)

Fig. 12. Augmented inputs and its estimated values in the adaptive sliding mode controller with uncertainty and sensor noise.

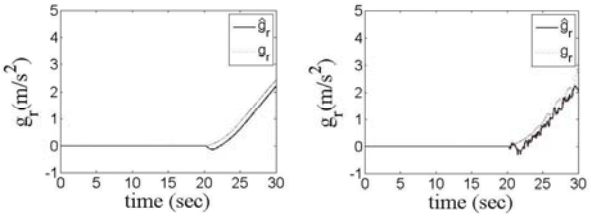

(a) Without sensor noise. (b) With sensor noise.

Fig. 13. Ground effect and its estimated values in the adaptive sliding mode controller.

As we can see in the Figs. 12 and 13, the adaptive sliding mode controller achieved good estimates of the auxiliary inputs and the ground effect both with and without the sensor noise, so that the control of the UAV could be done more precisely during landing.

6. CONCLUSIONS

In this paper, two types of nonlinear controllers were presented for a quadrotor helicopter. A feedback linearization (FL) controller was derived in a conventional way, with simplified dynamics to reduce the number of higher-order derivative terms involved in the design process. This controller uses control inputs that are very sensitive to sensor noise, because up to the third-order derivatives of state variables are included in the inputs. The FL controller is not robust to uncertainty as well as sensor noise. As an alternative, we introduced a new approach for the adaptive sliding mode controller using input augmentation to overcome the underactuated properties of the quadrotor helicopter. The inputs of the proposed sliding mode controller contain only the first derivatives of state variables and second derivatives of desired states. With a noise filter and saturation function, this controller performs well under sensor noise. Furthermore, the uncertainty caused by the ground effect can be compensated with a proper adaptation rule under the adaptive sliding mode control.

REFERENCES

[1] S. Bouabdallah, P. Murrireri, and R. Siegwart, "Design and control of an indoor micro quadrotor," *Proc. of the IEEE International Conference on Robotics and Automation*, pp. 4393-4398, 2004.

[2] B. Bluteau, R. Briand, and O. Patrouix, "Design and control of an outdoor autonomous quadrotor powered by a four strokes RC engine," *Proc. of IEEE Industrial Electronics, the 32nd Annual Conference*, pp. 4136-4141, 2006.

[3] E. Altug, J. P. Ostrowski, and R. Mahony, "Control of a quadrotor helocopter using visual feedback," *Proc. of the IEEE International Conference on Robotics and Automation*, vol. 1, pp. 72-77. 2002.

[4] E. Altug, J. P. Ostrowski, and C. J. Taylor, "Quadrotor control using dual camera visual feedback," *Proc. of the IEEE International Conference on Robotics and Automation*, vol. 3, pp. 4294-4299, 2003.

[5] T. Madani and A. Benallegue, "Control of a quadrotor mini-helicopter via full state backstepping technique," *Proc. of the 45th IEEE Conference on Decision and Control*, pp. 1515-1520, 2006.

[6] T. Madani and A. Benallegue, "Backstepping sliding mode control applied to a miniature quadrotor flying robot," *Proc. of IEEE Industrial Electronics, the 32nd Annual Conference*, pp. 700-

705, 2006.
[7] P. Castillo, P. Albertos, P. Garcia, and R. Lozano, "Simple real-time attitude stabilization of a quadrotor aircraft with bounded signals," *Proc. of the 45th IEEE Conference on Decision and Control*, pp. 1533-1538, 2006.
[8] N. Metni and T. Hamel, "Visual tracking control of aerial robotic systems with adaptive depth estimation," *International Journal of Control, Automation, and Systems*, vol. 5, no. 1, pp. 51-60, 2007.
[9] A. Benallegue, A. Mokhtari, and L. Fridman, "Feedback linearization and high order sliding mode observer for a quadrotor UAV," *Proc. of the International Workshop on Variable Structure Systems*, pp. 365-372, 2006.
[10] A. Tayebi and S. McGilvray, "Attitude stabilization of a VTOL quadrotor aircraft," *IEEE Trans. on Control Systems Technology*, vol. 14, no. 3, pp. 562-571, 2006.
[11] S. Bouabdallah, A. Noth, and R. Siegwart, "PID vs LQ control techniques applied to an indoor micro quadrotor," *Proc. of the IEEE/RJS International Conference on Intelligent Robots and Systems*, vol. 3, pp. 2451-2456, 2004.
[12] B. Erginer and E. Altug, "Modeling and PD control of a quadrotor VTOL vehicle," *Proc. of the IEEE Intelligent Vehicles Symposium*, pp. 894-899, 2007.
[13] L. Besnard, Y. Shtessel, and B. Landrum, "Control of a quadrotor vehicle using sliding mode disturbance observer," *Proc. of the American Control Conference*, pp. 5230-5235, 2007.
[14] C. Coza and C. J. B. Macnab, "A new robust adaptive-fuzzy control method applied to quadrotor helicopter stabilization," *NAFIPS Annual meeting of the North American Fuzzy Information Society*, pp. 454-458, 2006.
[15] A. Mokhtari, A. Benallegue, and B. Daachi, "Robust feedback linearization and controller for a quadrotor unmanned aerial vehicle," *Proc. of the IEEE/RSJ International Conference on Intelligent Robots and Systems*, pp. 1009-1014, 2005.
[16] A. Mokhtari and A. Benallegue, "Dynamic feedback controller of Euler angles and wind parameters estimation for a quadrotor unmanned aerial vehicle," *Proc. of the IEEE International Conference on Robotics and Automation*, pp. 2359-2366, 2004.
[17] R. Xu and U. Ozguner, "Sliding mode control of a quadrotor helicopter," *Proc. of the 45th IEEE Conference on Decision and Control*, pp. 4957-4962, 2006.
[18] S. Sastry, *Nonlinear Systems: Analysis, Stability, and Control*, Springer-Verlag, New York, NY, 1999.
[19] R. Prouty, *Helicopter Performance, Stability*, *and Control*, Krieger Pub. Co., 1995.

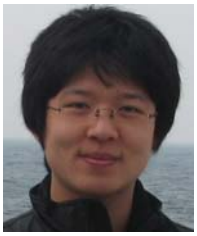

Daewon Lee received the B.S. degree in Mechanical and Aerospace Engineering from Seoul National University (SNU), Seoul, Korea, in 2005, where he is currently working toward a Ph.D. degree in Mechanical and Aerospace Engineering. He has been a member of the UAV research team at SNU since 2005. His research interests include applications of nonlinear control and vision-based control of UAV.

H. Jin Kim received the B.S. degree from Korea Advanced Institute of Technology (KAIST) in 1995, and the M.S. and Ph.D. degrees in Mechanical Engineering from University of California, Berkeley in 1999 and 2001, respectively. From 2002-2004, she was a Postdoctoral Researcher and Lecturer in Electrical Engineering and Computer Science (EECS), University of California, Berkeley (UC Berkeley). From 2004-2009, she was an Assistant Professor in the School of in Mechanical and Aerospace Engineering at Seoul National University (SNU), Seoul, Korea, where she is currently an Associate Professor. Her research interests include applications of nonlinear control theory and artificial intelligence for robotics, motion planning algorithms.

Shankar Sastry received the B.Tech. degree from the Indian Institute of Technology, Bombay, in 1977, and the M.S. degree in EECS, the M.A. degree in mathematics, and the Ph.D. degree in EECS from UC Berkeley, in 1979, 1980, and 1981, respectively. He is currently Dean of the College of Engineering at UC Berkeley. He was formerly the Director of the Center for Information Technology Research in the Interest of Society (CITRIS). He served as Chair of the EECS Department from January, 2001 through June 2004. In 2000, he served as Director of the Information Technology Office at DARPA. From 1996 to 1999, he was the Director of the Electronics Research Laboratory at Berkeley (an organized research unit on the Berkeley campus conducting research in computer sciences and all aspects of electrical engineering). He is the NEC Distinguished Professor of Electrical Engineering and Computer Sciences and holds faculty appointments in the Departments of Bioengineering, EECS and Mechanical Engineering. Prior to joining the EECS faculty in 1983 he was a Professor with the Massachusetts Institute of Technology (MIT), Cambridge. He is a member of the National Academy of Engineering and Fellow of the IEEE.